SHEP-08-31
March 3, 2009

One-loop Electro-Weak Corrections to the Event Orientation of $e^+e^- \to 3$ jet Processes[1]

C.M. Carloni-Calame[1], S. Moretti[1], F. Piccinini[2] and D.A. Ross[1]

[1] *School of Physics and Astronomy, University of Southampton Highfield, Southampton SO17 1BJ, UK*

[2] *INFN - Sezione di Pavia, Via Bassi 6, 27100 Pavia, Italy*

Abstract

We compute the full one-loop Electro-Weak (EW) contributions of $\mathcal{O}(\alpha_{\rm S}\alpha^3_{\rm EM})$ entering the electron-positron into a quark-antiquark pair plus one gluon cross section at the Z peak and LC energies in presence of polarisation of the initial state and by retaining the event orientation of the final state. We include both factorisable and non-factorisable virtual corrections, photon bremsstrahlung but not the real emission of $W^\pm$ and Z bosons. Their importance for the final state orientation is illustrated for beam polarisation setups achieved at SLC and foreseen at ILC and CLIC.

1 Introduction

There are innumerable tests of Quantum Chromo-Dynamics (QCD) that the $e^+e^- \to q\bar{q}g$ cross section can enable: it provides direct evidence for the existence of the gluon (the QCD gauge boson), it also allows one to measure its spin and to confirm its non-abelian nature, it permits the measurement of the QCD coupling constant ($\alpha_{\rm S}$), it is sensitive to the Casimir form factors of QCD. Furthermore, if the flavour of the final state quark can be tagged (as can efficiently be done for the case of b-quarks, thanks to μ-vertex or high-p_T lepton techniques), one can use $e^+e^- \to b\bar{b}g$ samples to verify the flavour independence of $\alpha_{\rm S}$ and to measure the b-quark (running) mass.

Thorough tests of QCD have been performed over the years and at many colliders (PETRA, TRISTAN, SLC/LEP and LEP2 [1]) through $e^+e^- \to q\bar{q}g$ and many more are foreseen at future ones, such as the ILC [2] or CLIC [3]. In fact, old $e^+e^- \to q\bar{q}g$ data are currently been revisited [4] in the light of the recently available Next-to-Next-to-Leading-Order NNLO QCD corrections [5], which can now supplement the NLO results of [6] (see

[1]Work supported in part by the U.K. Science and Technology Facilities Council (STFC).

also Refs. [7]–[9] for their implementation in numerical programs). However, as already emphasised in Refs. [10, 11], if $\mathcal{O}(\alpha_{\rm S}^3\alpha_{\rm EM}^2)$ results (NNLO QCD) are of experimental relevance, so are those of $\mathcal{O}(\alpha_{\rm S}\alpha_{\rm EM}^3)$ (NLO EW), since at the energies of the aforementioned colliders, $\mathcal{O}(\alpha_{\rm S}^2) \approx \mathcal{O}(\alpha_{\rm EM})$.

If full event orientation is retained in $e^+e^- \to q\bar{q}g$, one can further study certain polar and azimuthal angle asymmetries, which are strongly sensitive to parity-violating effects and thus represent a new search-ground for anomalous contributions that can be explored experimentally [12]–[14]. Such asymmetries are observed if beam polarisation can be exploited, as was the case at SLC and will certainly be possible at the ILC and CLIC. Finally, in the presence of polarised electrons and/or positrons, left-right asymmetries can also be studied. In these respects, while NLO and NNLO QCD effects can be the source of non-trivial asymmetry effects, one expects genuine parity-violating ones to occur naturally in NLO EW corrections. It is the purpose of this note to show that this is indeed the case, and at a sizable level given current experimental uncertanties, in both the unpolarised and polarised $e^+e^- \to q\bar{q}g$ cross section.

The paper is organised as follows. Section 2 briefly describes our calculation. Section 3 presents our numerical results whilst Section 4 summarises our main conclusions.

2 Calculation

The procedures adopted to carry out our computation have been described in the first paper of [11], to which we refer the reader for the most technical details. Here, we would only like to point out that, in anticipation of an electron-positron collider in which either or both the incoming beams can be polarised, we have inserted a helicity projection operator into the electron line and obtained separate results for left-handed (e_L) and right-handed (e_R) incoming electrons[2]. As already intimated in the Introduction, for genuinely weak interaction terms, this is of particular interest, since such corrections violate parity conservation. Unfortunately, this occurs already at tree-level [12], owing to the contribution from exchange of a Z boson, but these higher order corrections are also peculiarly dependent on the incoming lepton helicity and thus one would expect the two parity-violating effects be distinguishable after the collection of sufficient events. Also notice that, as well as the electron/positron mass, we also have neglected the masses of the quarks throughout. However, whenever there is a $W^\pm$ boson in the virtual loops, account has to be taken of the mass of the virtual top (anti)quark, which we have done.

Before proceeding to show our results, we should mention the numerical parameters used for our simulations. We have taken the top (anti)quark to have a mass $m_t = 171.6$ GeV. The Z mass used was $M_Z = 91.18$ GeV and was related to the $W^\pm$ mass, M_W, via the Standard Model (SM) formula $M_W = M_Z \cos\theta_W$, where $\sin^2\theta_W = 0.222478$. The Z width

[2]As we are taking massless incoming fermions, the helicity of the positron is simply the opposite to that of the electron.

was $\Gamma_Z = 2.5$ GeV. Also notice that, where relevant, Higgs contributions were included with $M_H = 115$ GeV. For the strong coupling constant, $\alpha_{\rm S}$, we have used the two-loop expression with $\Lambda_{\rm QCD}^{(n_f=4)} = 0.325$ GeV in the $\overline{\rm MS}$ scheme, yielding $\alpha_{\rm S}^{\overline{\rm MS}}(M_Z^2) = 0.118$.

As for the jet definition, partonic momenta are clustered into jets according to the Cambridge jet algorithm [16] (e.g., when $y_{ij} < y_{cut}$ with $y_{cut} = 0.001$), the jets are required to lie in the central detector region $30^\circ < \theta_{\rm jets} < 150^\circ$ and we require that the invariant mass of the jet system $M_{q\bar{q}g}$ is larger than $0.75 \times \sqrt{s}$. If a real photon is present in the final state, it is clustered according to the same algorithm, but we require that at least three "hadronic" jets are left at the end (i.e., events in which the photon is resolved are rejected)[3].

We will look at the cases of: (i) fully inclusive cross section, where no parton state can be identified from the jets; (ii) semi-inclusive cross section, where, e.g., the quark is assumed to be tagged and the gluon is taken to be the least energetic jet in the event; (iii) (fully) exclusive cross section, where each parton can be identified with a jet. Recall that, al least in the case of b-quarks, both the flavour (e.g., via a μ-vertex device) and charge (e.g., via the emerging lepton charge or the jet-charge method) of a quark can be extracted from a jet. (In all such cases, for sake of illustration, we take the efficiency to be unity.)

In order to show the behaviour of the EW corrections we are calculating, other than scanning in the collider energy, we have considered here the three discrete values of $\sqrt{s} = M_Z$ (for LEP/SLC, but also in view of a GigaZ option of a future LC), $\sqrt{s} = 350$ (the $t\bar{t}$ threshold of a ILC and/or CLIC) GeV and $\sqrt{s} = 1$ TeV (as representative of the so-called 'Sudakov regime' [15] which can be realised at both ILC and CLIC). For reference, concerning beam polarisation, we will adopt 70% electron polarisation at $\sqrt{s} = M_Z$ (thus emulating the SLC configuration) and 100% at $\sqrt{s} = 350$ GeV and 1 TeV (thus emulating a possible ILC/CLIC configuration)[4].

3 Numerical Results

Before proceeding to investigate the spatial orientation of the $e^+e^- \to q\bar{q}g$ differential cross section through the $\mathcal{O}(\alpha_{\rm S}\alpha_{\rm EM}^3)$ in presence of one-loop EW corrections of $\mathcal{O}(\alpha_{\rm EM})$, it is instructive to see the effects of the various components of these corrections on the tree-level $\mathcal{O}(\alpha_{\rm S}\alpha_{\rm EM}^2)$ result for the integrated cross section, as a function of the collider energy. This is done in Fig. 1, for the two electron polarisations separately. The curves represent the effects of the QED (virtual and real) corrections only, the gauge bosons self-energy

[3]As explained in the first paper in [11], this serves a twofold purpose. On the one hand, from the experimental viewpoint, a resolved (energetic and isolated) single photon is never treated as a jet. On the other hand, from a theoretical viewpoint, this enables us to remove divergent contributions appearing whenever an unresolved (soft and/or collinear) gluon is emitted, since we are not computing here the one-loop $\mathcal{O}(\alpha_{\rm S}\alpha_{\rm EM}^3)$ QCD corrections to $e^+e^- \to q\bar{q}\gamma$.

[4]Recall that, in our case, since we take all external fermions to be massless, the positron has opposite helicity to that of the electron.

corrections, the non-factorisable graphs involving four- and five-point functions with WW exchange[5], the weak corrections with the non-factorisable WW graphs removed and the sum of the previous ones. Notice that the total effect depends strongly on the electron polarisation state. If the electron is right-handed, there are no contributions from the non-factorisable WW graphs. Furthermore, there are strong cancellations between the gauge bosons self-energy terms (which are increasingly positive) and the full weak corrections with the non-factorisable WW graphs omitted, (which are increasingly negative). Here, the QED terms are never very large. Overall, the full $\mathcal{O}(\alpha_{\rm EM})$ correction is small, as it is always below the -2% level. In contrast, overall effects are very large in the case of left-handed electrons, also displaying the typical Sudakov enhancement at large energies: e.g., at 1 TeV, the full $\mathcal{O}(\alpha_{\rm EM})$ correction can reach -20%. Here, the dominant terms, again of opposite signs, are the full weak minus non-factorisable WW component (increasingly positive) and the non-factorisable WW terms (increasingly negative), with the QED effects being at the (positive) percent level and the gauge boson self-energies yielding up to $+25\%$ corrections.

We start our differential analysis by assuming a fully inclusive setup, whereby jets are labelled only in terms of their energies, $E_3 \leq E_2 \leq E_1$, and the event orientation is identified uniquely by adopting as polar and azimuthal variables (see Ref. [12]) those defined as the angle of the fastest jet with respect to the electron beam direction (denoted by θ_{ij}) and the one whose cosine satisfies (with obvious meaning of the vector symbols)

$$\cos\chi'' = \frac{\vec{1}\times\vec{3}}{|\vec{1}\times\vec{3}|}\cdot\frac{\vec{1}\times\vec{e^-}}{|\vec{1}\times\vec{e^-}|}, \tag{1}$$

respectively. At the Z pole, EW corrections of $\mathcal{O}(\alpha_{\rm EM})$ to the polar angle are substantial, up to -40% at fixed order and dominated by the QED component, as the purely weak part, involving only the exchange of $W^\pm$ and/or Z bosons, accounts only for a -5% or so. The QED effects are tamed by the inclusion of even higher order Leading Logarithmic (LL) effects (see [11] for the details of the implementation), though they decrease only slightly, to -35%. Such large effects are mainly driven by the Initial State Radiation (ISR) affecting the line-shape of the cross section around the resonance and are essentially independent of the polarisation state of the electron. With increasing collider energy, for the case of left-handed electrons, the overall corrections diminish in absolute size, to no more than -25% (at $\sqrt{s} = 1$ TeV), even becoming positive in the forward/backward directions. Such a decrease affects the QED component. At the same time, owing to the onset of the Sudakov regime, the effects due to the weak component of the $\mathcal{O}(\alpha_{\rm EM})$ corrections increase in size, to -15% or so at 1 TeV (in the central region). In contrast with the case of low energy, for high values of $\sqrt{s}$, the $\mathcal{O}(\alpha_{\rm EM})$ effects induced by right-handed electrons are different, being smaller by about factor of 3 when the corrections are negative and larger by about a factor of 3 when the corrections are positive, for both $\sqrt{s} = 350$ GeV and $\sqrt{s} = 1$ TeV. For

[5]This is a gauge invariant subset of the complete corrections.

the $\mathcal{O}(\alpha_{\rm EM})$ purely weak part, for right-handed electrons, it can be seen that corrections become positive and somewhat smaller, in this case independent of whether the collider energy is at the $t\bar{t}$ threshold or in the TeV regime. We display all these patterns in Figs. 2–4.

Unlike the case of the polar angle, the corrections to the differential cross sections with resepct to the azimuthal angle at the Z peak are essentially flat. Their hierarchy and size, however, are the same for both variables. In fact, at fixed $\mathcal{O}(\alpha_{\rm EM})$, QED corrections are always the leading ones whilst the weak effects are subleading, the former being a factor of 9 or so larger than the latter, both being negative and summing up to -45%. LL resummation effects in QED reduce the overall corrections to -40%. Again, at this low energy, there is no dependence of the $\mathcal{O}(\alpha_{\rm EM})$ EW effects on the electron polarisation. As $\sqrt{s}$ increases, QED effects are no longer constant, as they are maximal (and negative) for $\chi'' = 90^{\rm o}$, about $-15\%(-5\%)$ at 350 GeV and $-20\%(-5\%)$ at 1 TeV, for left-handed(right-handed) electrons, with minimal effects due to the QED LL resummation. The purely weak corrections are instead constant throughout the entire angular range, approximately $-6\%(-8\%)[-12\%]$ at $\sqrt{s} = M_Z(350$ GeV$)[1$ TeV$]$, for left-handed electrons. For right-handed ones, the corresponding numbers are $-9\%(+2\%)[+3\%]$ or so. All this is shown in Figs. 5–7.

In the semi-inclusive case we found little differences with respect to the fully inclusive setup in the case of both the polar and azimuthal angles, hence we will not dwell upon these variables here. This is also true for the polar angle in the case of the exclusive analysis, so that we do not treat this variable either. In contrast, the azimuthal distribution, which we now define as (again, with obvious meaning of the vector symbols)

$$\cos\chi = \frac{\vec{q}\times\vec{g}}{|\vec{q}\times\vec{g}|}\cdot\frac{\vec{q}\times\vec{e^-}}{|\vec{q}\times\vec{e^-}|}, \tag{2}$$

is affected somewhat differently in the exclusive case compared with the fully inclusive one. This is displayed in Figs. 8–10. Whilst at $\sqrt{s} = M_Z$ differences between these two cases are really minimal and, in fact, mainly due to the shape of the tree-level distributions, at $\sqrt{s} = 350$ GeV and 1 TeV, the $\mathcal{O}(\alpha_{\rm EM})$ effects are different in both shape and size. Whilst the QED ones still display a maximum (negative) correction at $\chi = 90^{\rm o}$, they also show local maxima (either positive or negative) in the near forward/backward directions, for both energies and both electron polarisations. Sizewise, in the exclusive case, QED corrections are smaller than in the fully inclusive case, with this reduction being more pronounced (by a factor of 3 or so) for right-handed rather than left-handed (by a factor of 1.5 or so) electrons. (Also notice that QED LL resummation effects through higher orders are never relevant.) Finally, the purely weak corrections in the exclusive case are never substantially different from the counterparts in the fully inclusive scenario.

4 Summary

In summary, a careful analysis of actual $e^+e^- \to q\bar{q}g$ events, involving one-loop EW effects, is required, particularly in presence of beam polarisation and high energy, if one wants to accurately characterise the event orientation. We have in fact found substantial $\mathcal{O}(\alpha_{\rm EM})$ corrections in the case of both the QED and weak components that render the full one-loop $\mathcal{O}(\alpha_{\rm S}\alpha_{\rm EM}^3)$ predictions measureably different from the tree-level $\mathcal{O}(\alpha_{\rm S}\alpha_{\rm EM}^2)$ ones for both polar and azimuthal angular distributions used to identify the event orientation, irrespective of the level of inclusiveness (or exclusiveness) of the analysis. Hence, since such genuine SM effects could well mimick new physics phenomena, it is of paramount importance that they are accounted for in phenomenological studies of the three-jet event sample. In our calculation, we have neglected tree-level $W^\pm$ and Z bremsstrahlung through $\mathcal{O}(\alpha_{\rm S}\alpha_{\rm EM}^3)$, as we expect that, in view of the cleanliness of three-jet samples produced in electron-positron machines compared with hadronic ones, their contribution can be efficiently identified and removed from the data.

References

[1] For reviews, see: H. Sagawa, in proceedings of the XXIXth Rencontres de Moriond, 19-26 March 1994, Les Arcs, Savoie, France (ed. J. Tran Thanh Van, Editions Frontieres, 1994) p. 69; S.L. Wu, Phys. Rep. **107** (1984) 59; S. Bethke, Eur. Phys. J. direct C **4** (2002) 1 and Phys. Rept. **403-404** (2004) 203; D. Muller et al. [SLD Collaboration], SLAC-PUB-8792 and Nucl. Phys. Proc. Suppl. **86** (2000) 7; K. Abe et al. [SLD Collaboration], arXiv:hep-ex/9910023.

[2] S. Bethke, *Prepared for 2nd International Workshop on Physics and Experiments with Linear e+ e- Colliders, Waikoloa, Hawaii, 26-30 Apr 1993.*

[3] E. Accomando et al. [CLIC Physics Working Group], arXiv:hep-ph/0412251.

[4] C. Pahl, S. Bethke, S. Kluth, J. Schieck [JADE Collaboration], arXiv:0810.2933 [hep-ex] and arXiv:0810.1389 [hep-ex].

[5] A. Gehrmann-De Ridder, T. Gehrmann, E.W.N. Glover and G. Heinrich, arXiv:0802.0813 [hep-ph]; arXiv:0801.2680 [hep-ph]; JHEP **0712** (2007) 094; JHEP **0711** (2007) 058; arXiv:0709.4221 [hep-ph]; arXiv:0709.1608 [hep-ph]; 0707.1285 [hep-ph]; Nucl. Phys. Proc. Suppl. **160** (2006) 190; A. Gehrmann-De Ridder, T. Gehrmann and E.W.N. Glover, Nucl. Phys. Proc. Suppl. **135** (2004) 97; L.W. Garland, T. Gehrmann, E.W.N. Glover, A. Koukoutsakis and E. Remiddi, Nucl. Phys. **B642** (2002) 227; Nucl. Phys. **B627** (2002) 107.

[6] R.K. Ellis, D.A. Ross and A.E. Terrano, Nucl. Phys. **B178** (1981) 421.

[7] See, e.g.: Z. Kunszt and P. Nason (conveners), in proceedings of the workshop 'Z Physics at LEP1' (G. Altarelli, R. Kleiss and C. Verzegnassi, eds.), preprint CERN-89-08, 21 September 1989 (and references therein).

[8] W. T. Giele and E. W. N. Glover, Phys. Rev. D **46** (1992) 1980.

[9] S. Catani and M. H. Seymour, Phys. Lett. B **378** (1996) 287.

[10] E. Maina, S. Moretti, M. R. Nolten and D. A. Ross, hep-ph/0407150; hep-ph/0403269; JHEP **04** (2003) 056.

[11] C. M. Carloni Calame, S. Moretti, F. Piccinini and D. A. Ross, arXiv:0804.3771 [hep-ph] (to appear in JHEP); C. M. Carloni Calame, S. Moretti, F. Piccinini and D. A. Ross, PoS **RADCOR2007** (2007) 004; C. M. C. Calame, S. Moretti, F. Piccinini and D. A. Ross, arXiv:0811.4758 [hep-ph].

[12] P. N. Burrows and P. Osland, Phys. Lett. B **400** (1997) 385; arXiv:hep-ph/9712312.

[13] J. G. Körner and G. A. Schuler, Z. Phys. C **26** (1985) 559; J. G. Körner, G. A. Schuler and F. Barreiro, Phys. Lett. B **188** (1987) 272.

[14] E. Laermann, K. H. Streng, P. M. Zerwas, Z. Phys. C **3** (1980) 289 [Erratum: Z. Phys. **C52** (1991) 352].

[15] P. Ciafaloni and D. Comelli, Phys. Lett. **B446** (1999) 278.

[16] Yu. L. Dokshitzer, G. D. Leder, S. Moretti and B. R. Webber, JHEP **08** (1997) 001; S. Moretti, L. Lönnblad and T. Sjöstrand, JHEP **08** (1998) 001.

[17] U. Baur, Phys. Rev. **D75** (2007) 013005.

[18] S. Moretti, M. R. Nolten and D. A. Ross, Phys. Rev. **D74** (2006) 097301; Phys. Lett. **B643** (2006) 86; Phys. Lett. **B639** (2006) 513 [Erratum, *ibidem* **B660** (2008) 607]; Nucl. Phys. **B759** (2006) 50; E. Maina, S. Moretti, M. R. Nolten and D. A. Ross, Phys. Lett. **B570** (2003) 205.

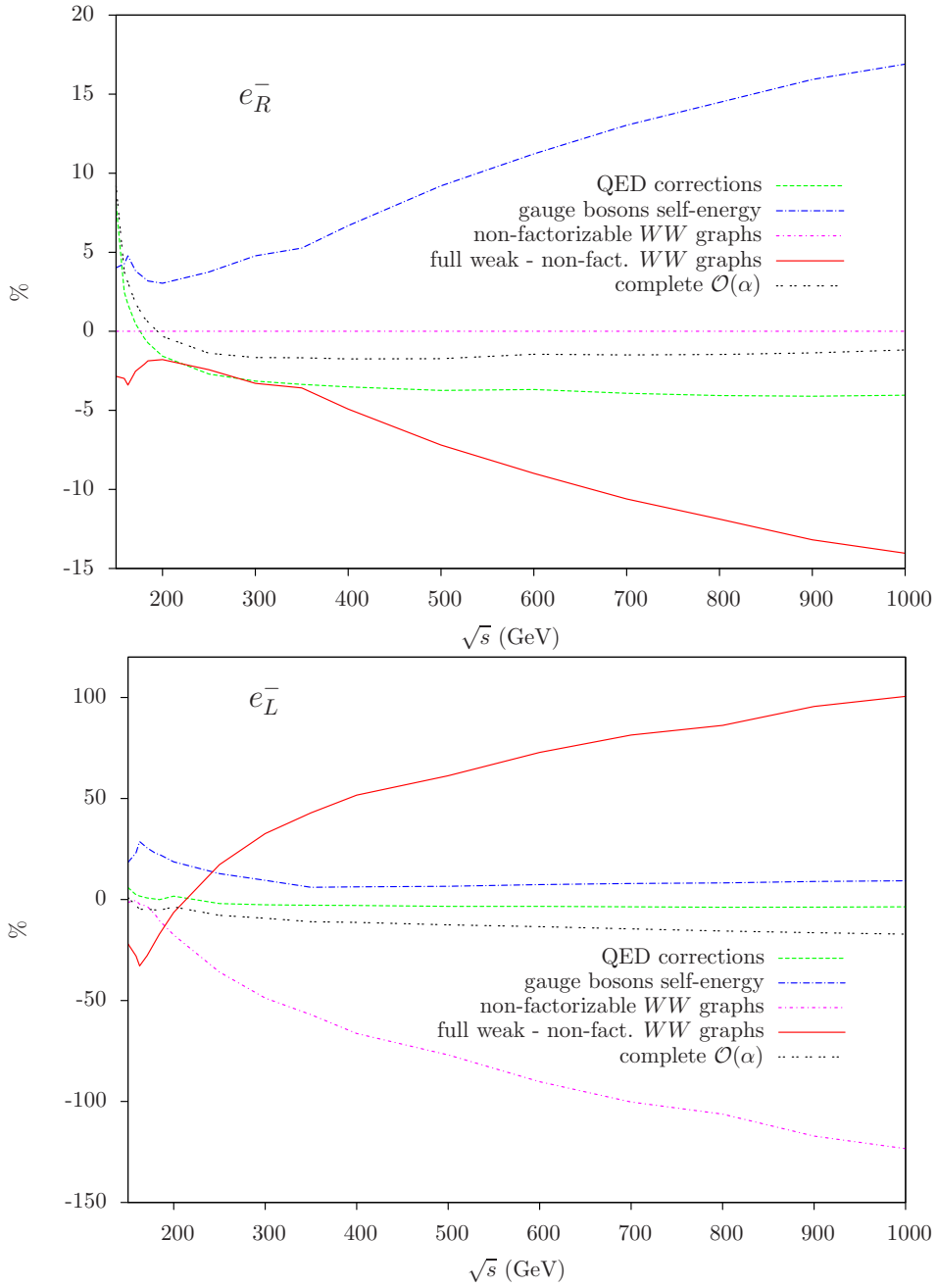

Figure 1: Top/Bottom is for e_R^-/e_L^-: Relative effect on the integrated cross section due to different contributions to the order $\alpha \equiv \alpha_{\rm EM}$ correction, as a function of the CM energy.

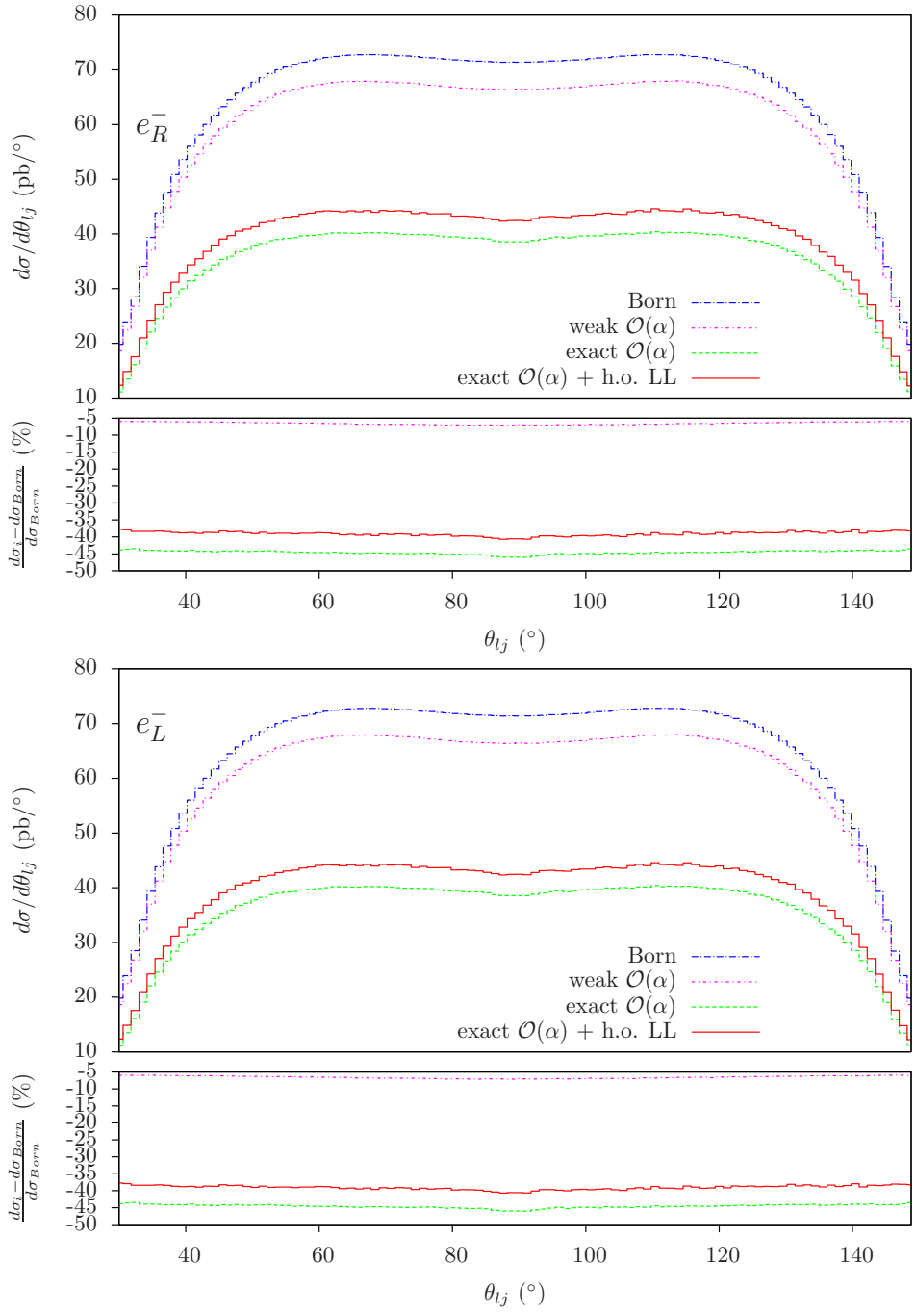

Figure 2: Top/Bottom is for e_R^-/e_L^-: $\frac{d\sigma}{d\theta_{lj}}$ distribution at the Z peak. (See the main text for the definition of this variable.)

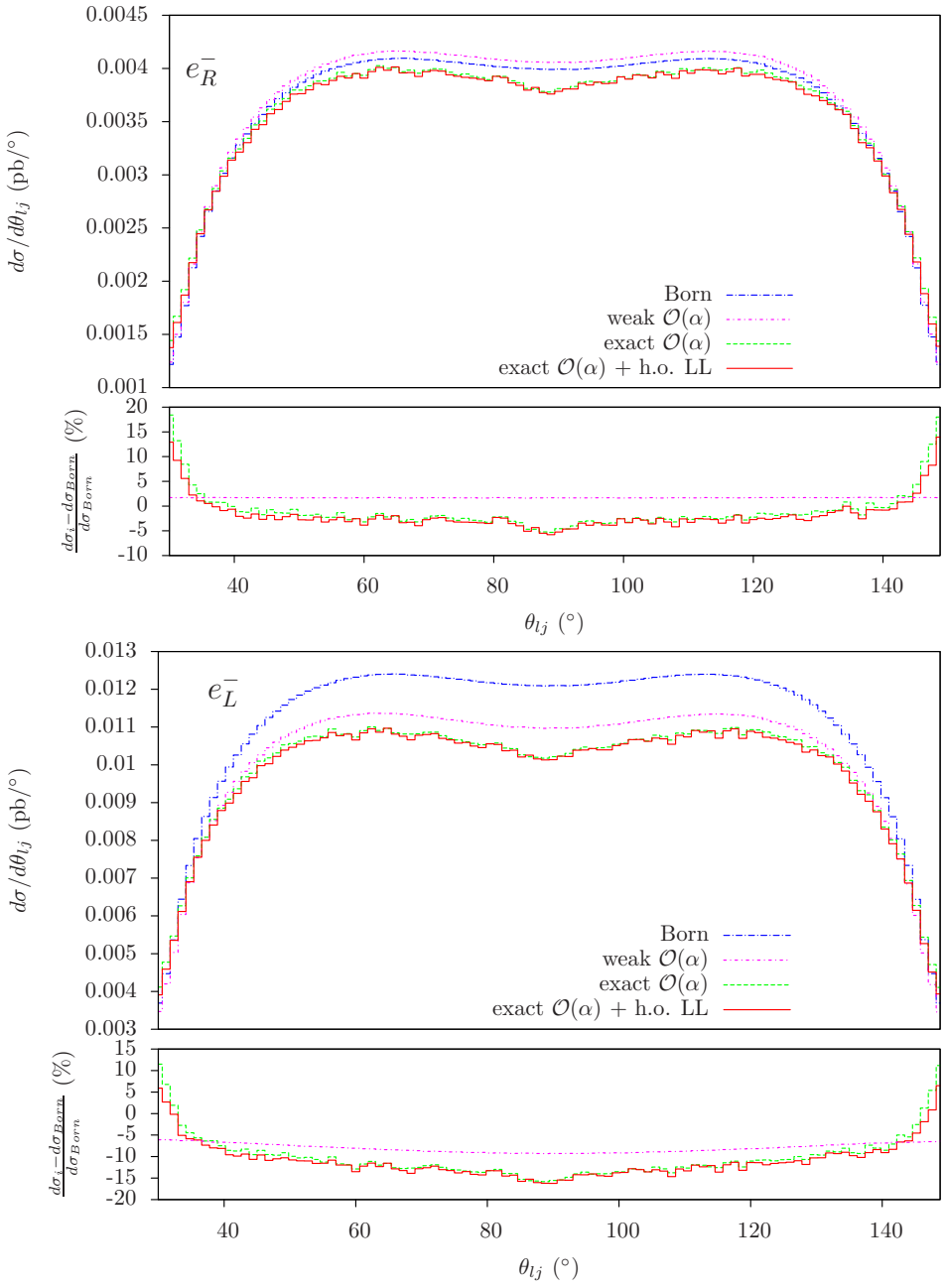

Figure 3: Top/Bottom is for e_R^-/e_L^-: $\frac{d\sigma}{d\theta_{lj}}$ distribution at 350 GeV. (See the main text for the definition of this variable.)

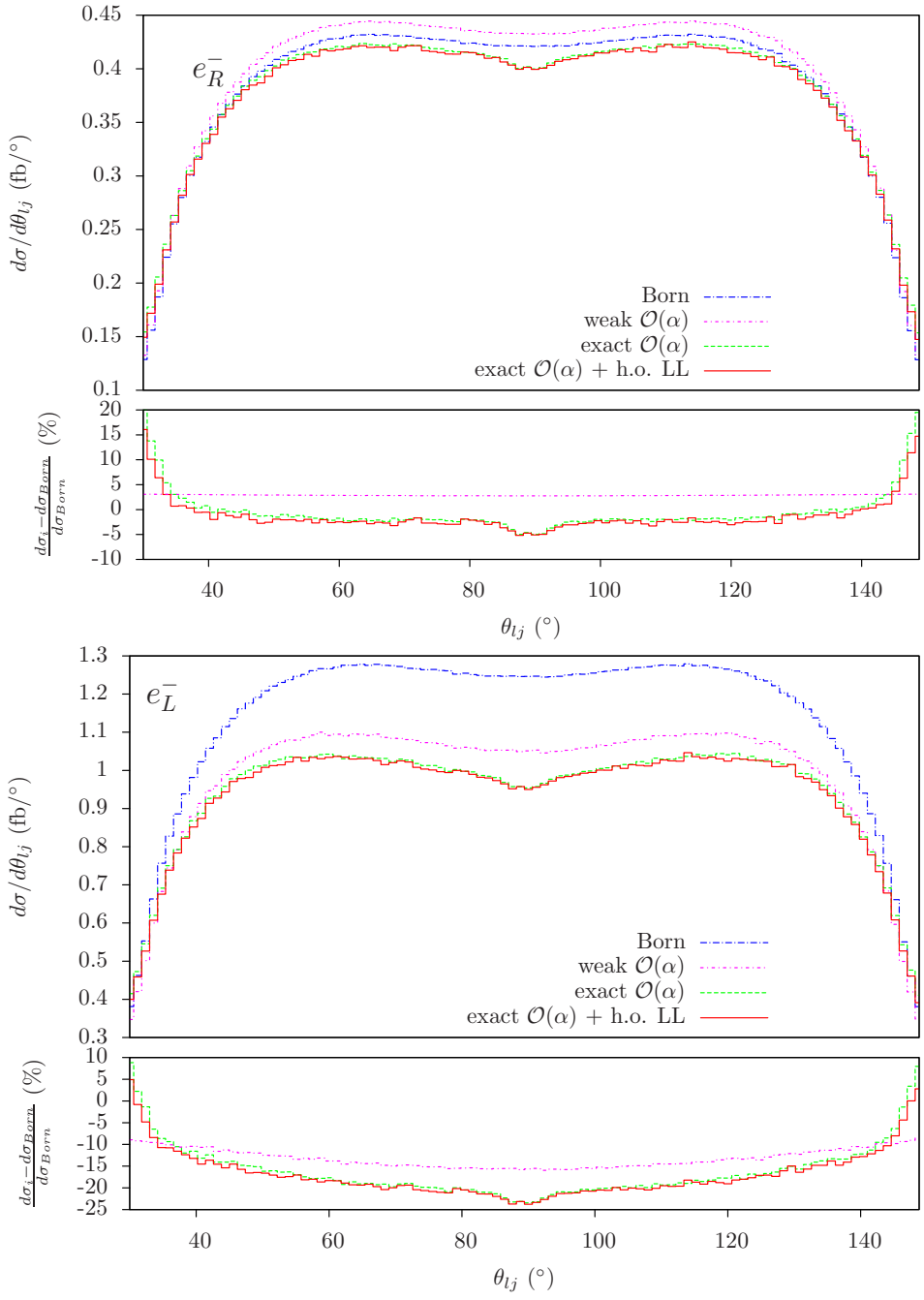

Figure 4: Top/Bottom is for e_R^-/e_L^-: $\frac{d\sigma}{d\theta_{lj}}$ distribution at 1 TeV. (See the main text for the definition of this variable.)

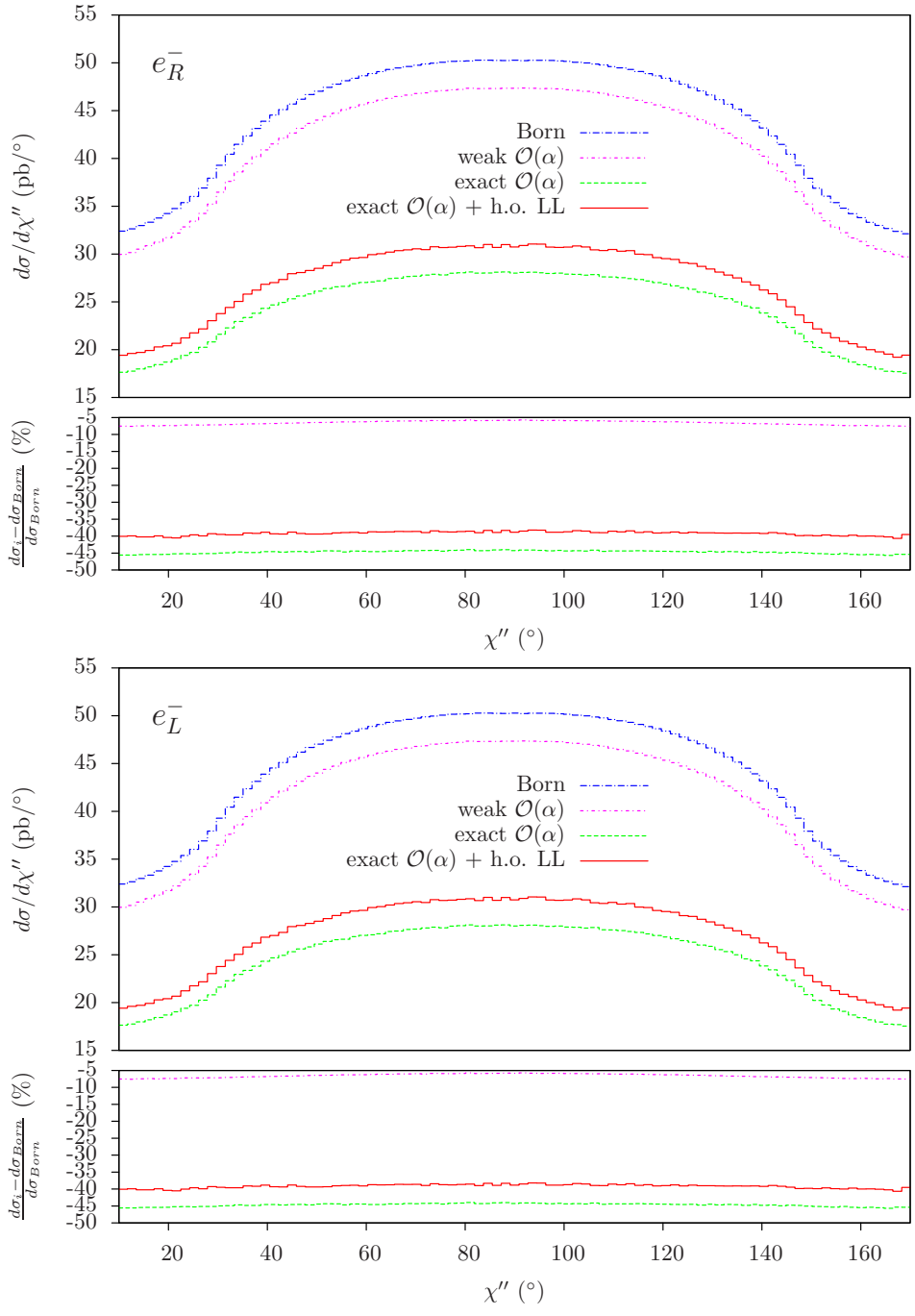

Figure 5: Top/Bottom is for e_R^-/e_L^-: $\frac{d\sigma}{d\chi''}$ distribution at the Z peak. (See the main text for the definition of this variable.)

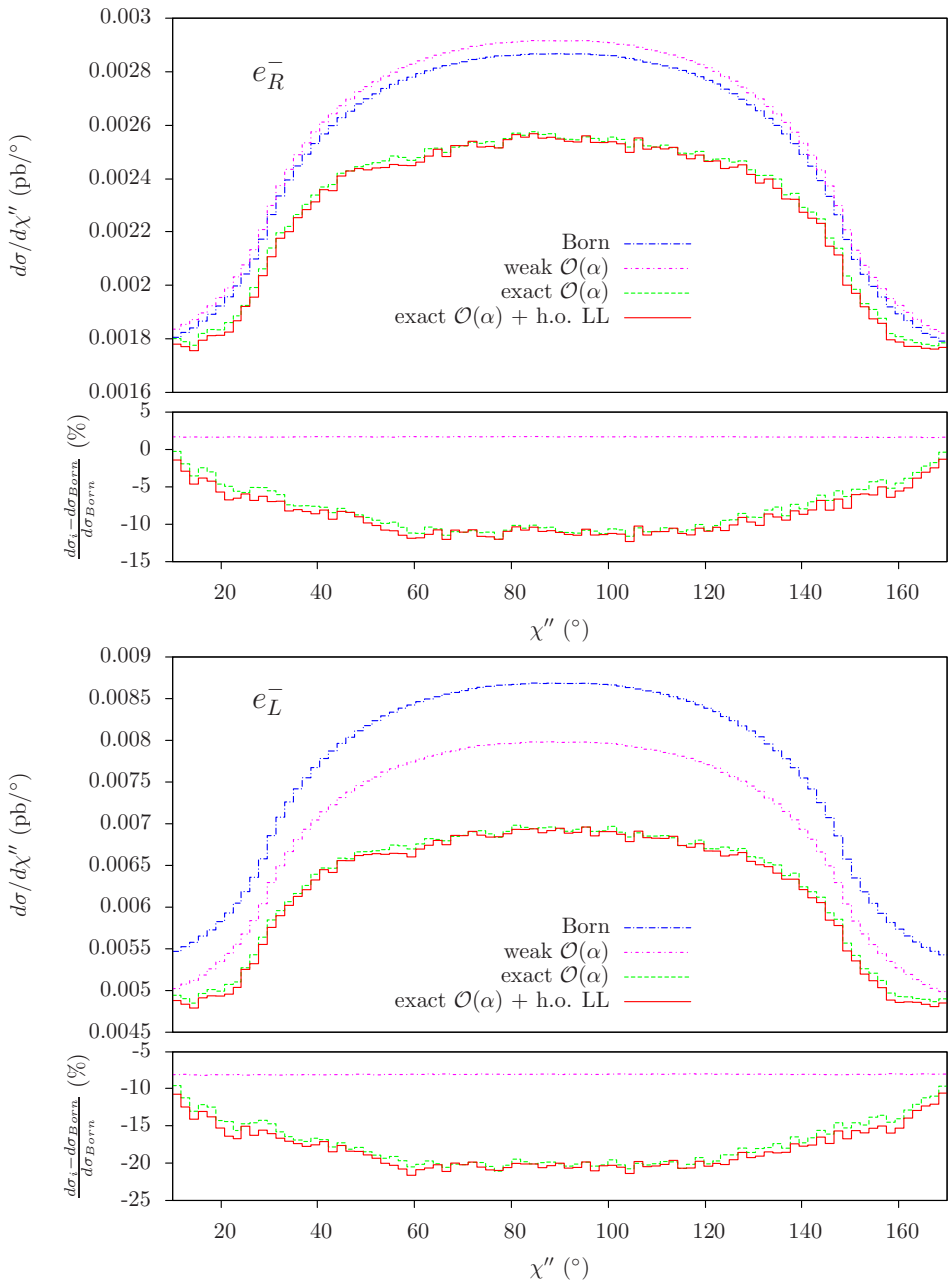

Figure 6: Top/Bottom is for e_R^-/e_L^-: $\frac{d\sigma}{d\chi''}$ distribution at 350 GeV. (See the main text for the definition of this variable.)

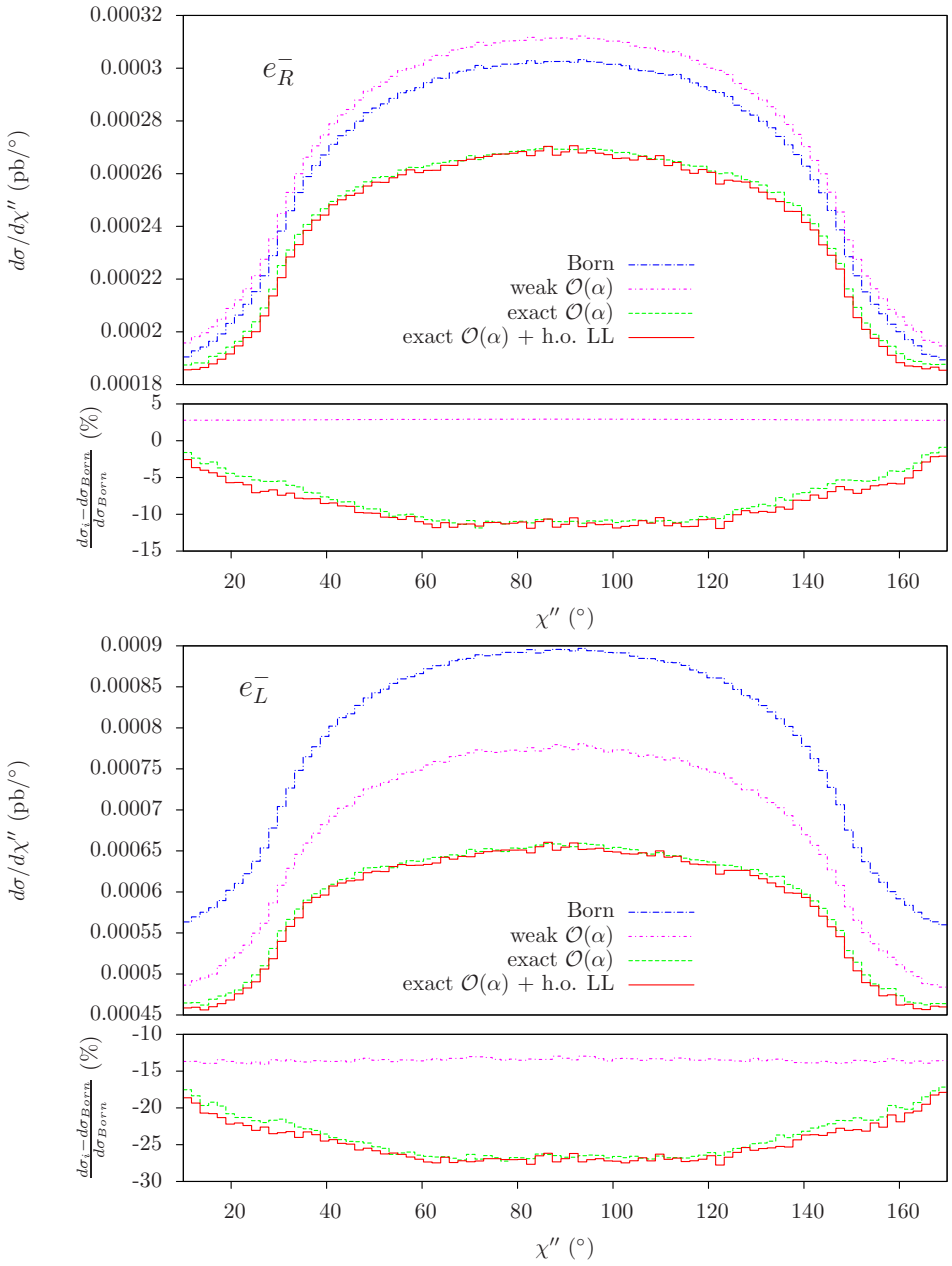

Figure 7: Top/Bottom is for e_R^-/e_L^-: $\frac{d\sigma}{d\chi''}$ distribution at 1 TeV. (See the main text for the definition of this variable.)

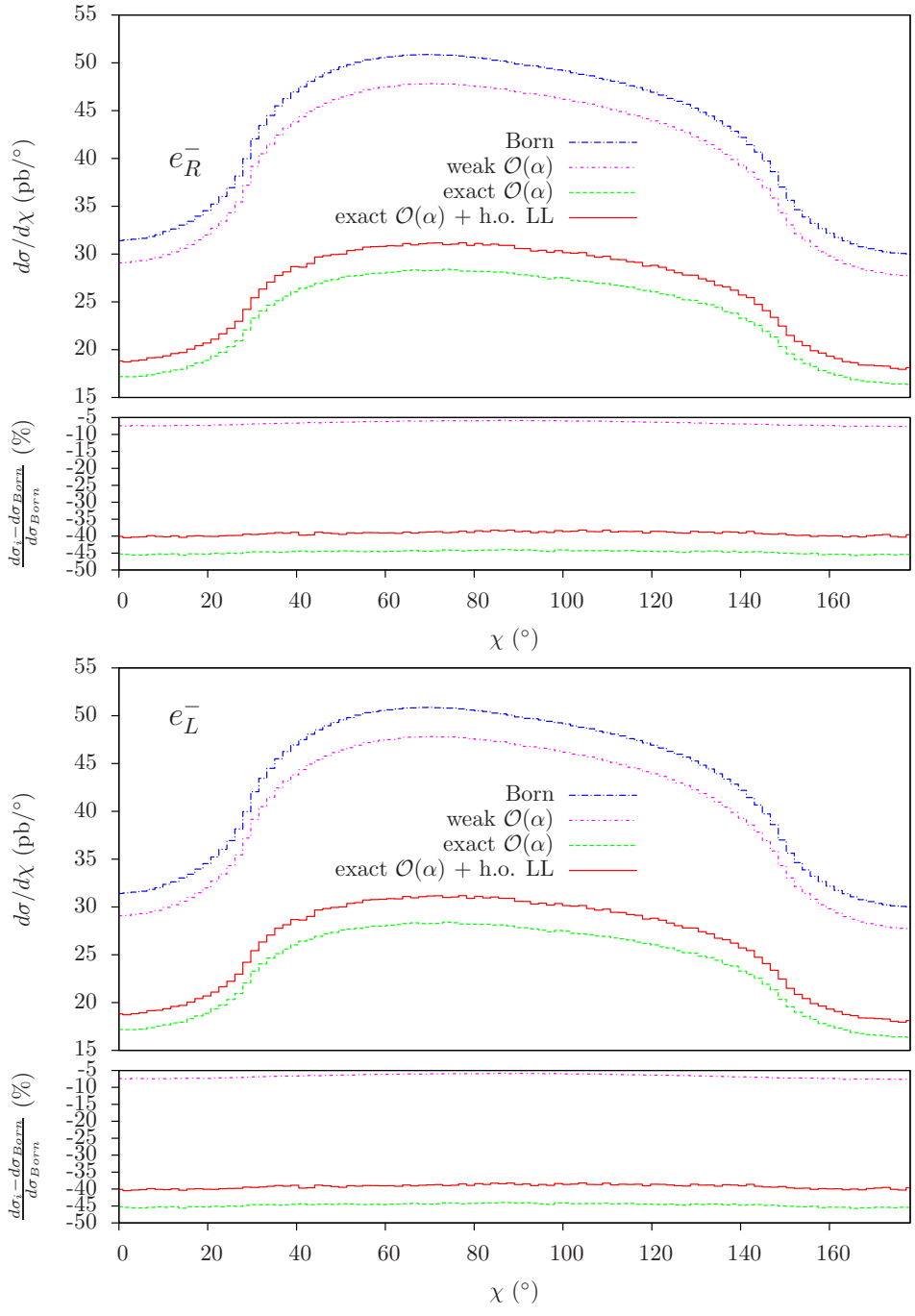

Figure 8: Top/Bottom is for e_R^-/e_L^-: $\frac{d\sigma}{d\chi}$ distribution at the Z peak. (See the main text for the definition of this variable.)

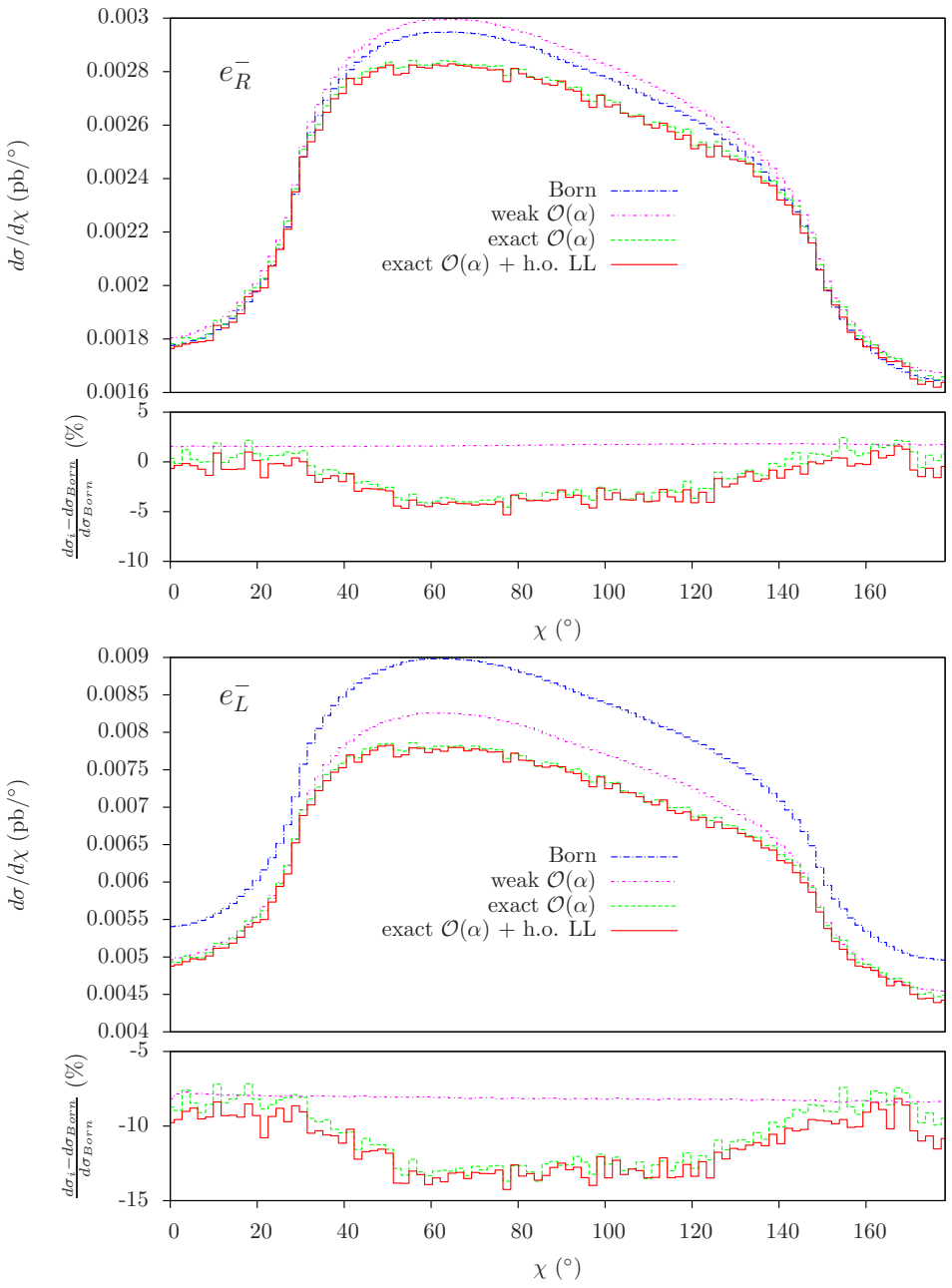

Figure 9: Top/Bottom is for e_R^-/e_L^-: $\frac{d\sigma}{d\chi}$ distribution at 350 GeV. (See the main text for the definition of this variable.)

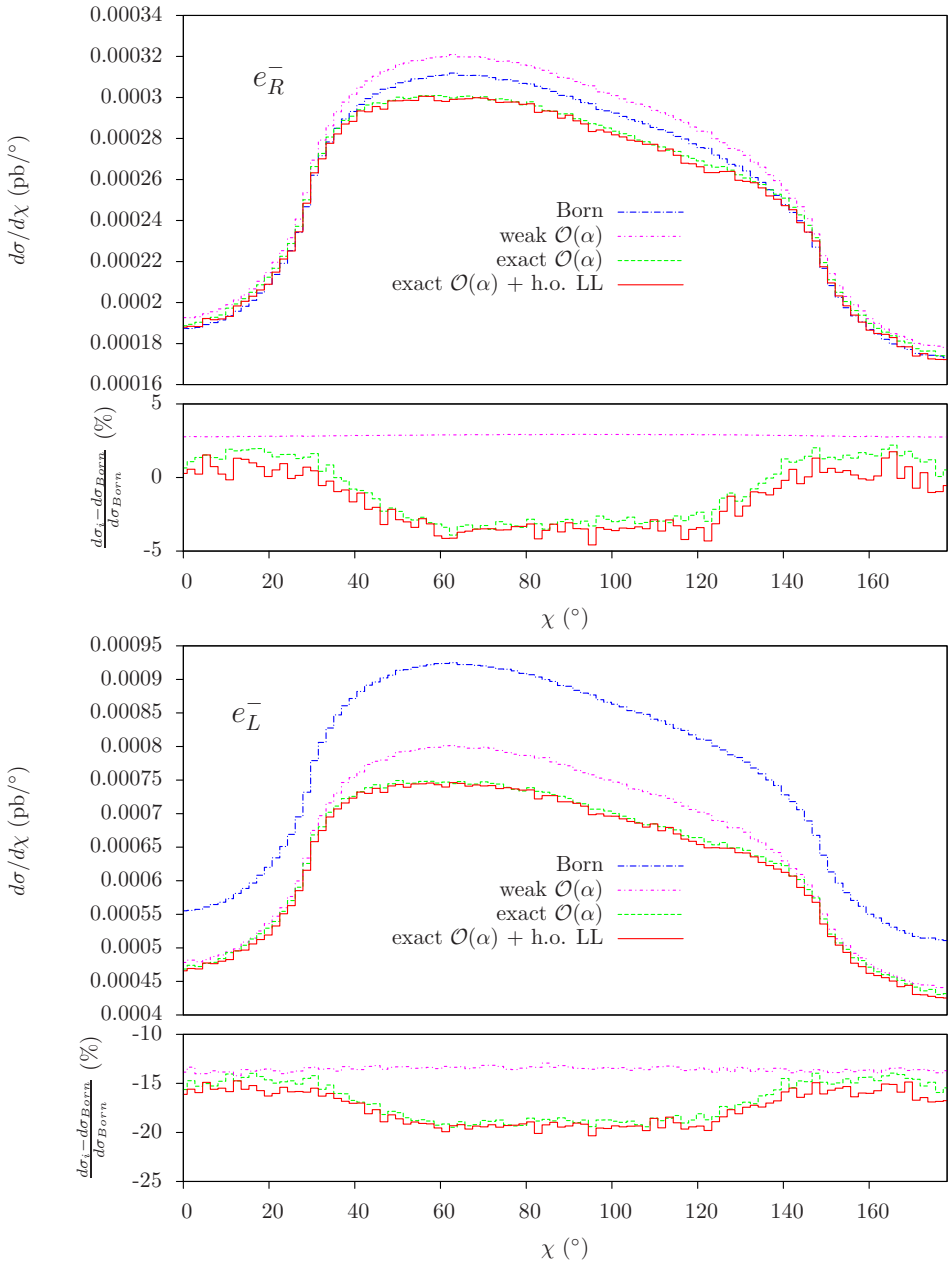

Figure 10: Top/Bottom is for e_R^-/e_L^-: $\frac{d\sigma}{d\chi}$ distribution at 1 TeV. (See the main text for the definition of this variable.)